Theoretical Analysis of a Ridged-Waveguide Mounting Structure

[5] H. P. Shuch, "1296 MHz transceiver," *Ham Radio*, pp. 8–23, Sept. 1974.
[6] ——, "UHF double balanced mixers," *Ham Radio*, pp. 8–15, July 1975.
[7] ——, "High performance conversion module for the 23-cm band," *Radio Handbook*, 20th ed. Indianapolis, IN: Howard Sams & Co., 1975, pp. 20–66.
[8] ——, "Solid state microwave amplifier design," *Ham Radio*, pp. 40–47, Oct. 1976.
[9] J. J. Nagle, "A method of converting the SMS/GOES WEFAX frequency (1691 MHz) to the existing APT/WEFAX frequency (137 MHz)," NOAA Tech. Memo. NESS 54, Apr. 1974.
[10] "Noise parameters and noise circles for the HXTR-6101, -6102, -6103, -6104, and -6105 low noise transistors," Application Bulletin 17, Hewlett-Packard Company, Jan. 1977.

Theoretical Analysis of a Ridged-Waveguide Mounting Structure

SHIZUO MIZUSHINA, MEMBER, IEEE,
NOBUO KUWABARA, MEMBER, IEEE,
AND HIROSHI KONDOH, MEMBER, IEEE

Abstract—**The driving-point impedance of a single-gap thin conductor strip, a model of the ribbon-and-pedestal of diode package, mounted across the gap of a ridged waveguide has been derived using the induced EMF method. The dyadic Green's function for the ridged waveguide is derived to facilitate the analysis. An equivalent circuit is developed which involves an infinite array of transformers representing the couplings between the conductor strip and the waveguide normal modes. Numerical results for a typical example are presented to discuss the validity of the analytical results and also to demonstrate a remarkably smooth behavior of the driving-point impedance of the mount over a frequency range from 5.4 to 25.4 GHz.**

Introduction

Ridged waveguides have been used for many years in microwave components and systems requiring broad bandwidths. Among such applications, mounting structures for solid-state devices are of our interest here [1], including the fin-line components [2]. A recent experimental investigation showed that mechanical tuning ranges of 8.5–26 GHz and 14–28 GHz were achieved with packaged Gunn and IMPATT diodes, respectively, mounted in the ridged-waveguide cavities [3], [4]. This gave us a motivation to study the ridged-waveguide mounting structure theoretically as well. An attempt was made to extend the induced EMF method, which had been successfully applied to the rectangular waveguide post-coupling structure [5], [6], to a ridged-waveguide mounting structure where a packaged diode fitted into the gap spacing between the ridges extending uniformly in the z direction. In this short paper we analyze a simplified model of the mount, in which the package ceramic ring is disregarded and the ribbon-and-pedestal of the diode is represented by an equivalent flat conductor strip, as in [5], [6], to derive its driving-point impedance.

Analysis

A cross section of the ridged-waveguide mounting structure is sketched in Fig. 1(a) and the model used in the analysis in Fig. 1(b) along with the coordinate system. The conductor strip with a width w, a gap g, and an infinitesimal thickness at $z = 0$ is regarded as a small antenna radiating into the ridged waveguide. The electric field in the guide $\boldsymbol{E}(\boldsymbol{R})$ generated by the current density $\boldsymbol{J}(\boldsymbol{R})$ in the conductor strip can be derived by

$$\boldsymbol{E}(\boldsymbol{R}) = -j\omega\mu_0 \int_{\text{vol}} \bar{\boldsymbol{G}}(\boldsymbol{R}/\boldsymbol{R}') \cdot \boldsymbol{J}(\boldsymbol{R}/\boldsymbol{R}')\, dv' \tag{1}$$

provided that the Green's function, $\bar{\boldsymbol{G}}(\boldsymbol{R}/\boldsymbol{R}')$, is known. It is possible to derive $\bar{\boldsymbol{G}}(\boldsymbol{R}/\boldsymbol{R}')$ for the ridged waveguide using the Ohm–Rayleigh method described by Tai in [7] with the aid of the knowledge of the complete eigenfunctions of the ridged waveguide given by Montgomery in [8]. Quoting from [8], we can write for the y component of the electric basis field in region 1, referring to Fig. 1(b), as

$$e_{Hy}(\boldsymbol{R}) = -\sum_{n=0}^{\infty} \eta_{1n} k_{x1n} \cos k_{x1n} x \cos \frac{n\pi}{b_3}(y - b_3) \tag{2}$$

for TE modes and

$$e_{Ey}(\boldsymbol{R}) = \sum_{n=1}^{\infty} \xi_{1n} \frac{n\pi}{b_3} \cos k_{x1n} x \cos \frac{n\pi}{b_3}(y - b_3) \tag{3}$$

for TM modes where k_{x1n} is defined by

$$k_{x1n} = \begin{cases} \sqrt{k_T^2 - \left(\frac{n\pi}{b_3}\right)^2}, & k_T \geq \frac{n\pi}{b_3} \\ -j\sqrt{\left(\frac{n\pi}{b_3}\right)^2 - k_T^2}, & k_T < \frac{n\pi}{b_3} \end{cases} \tag{4}$$

with

$$\Gamma = \begin{cases} \sqrt{k^2 - k_T^2}, & k \geq k_T \\ -j\sqrt{k_T^2 - k^2}, & k < k_T \end{cases} \tag{5}$$

and $k = \omega\sqrt{\varepsilon_0 \mu_0}$.

In the above expressions, we adopted the convention $\exp(j\omega t - j\Gamma z)$ for the wave propagating in the positive z direction and the subscripts H and E for the TE and the TM modes, respectively. In (2) and (3) we retained only those modes which satisfy the magnetic-wall-boundary condition at the symmetry plane of the waveguide since the current is centered at this plane. In (4), k_T is an eigenvalue and k_{x1n} is the propagation constant in the x direction of the spatial harmonic component in region 1 associated with the eigenvalue. The amplitudes of these spatial

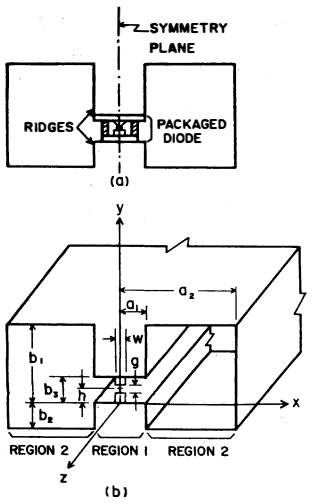

Fig. 1. A ridged-waveguide mounting structure. (a) A cross-sectional sketch of the mount. (b) The model used in the analysis.

Manuscript received May 13, 1977; revised July 22, 1977.

S. Mizushina and H. Kondoh are with The Research Institute of Electronics, Shizuoka University, Hamamatsu 432, Japan.
N. Kuwabara was with The Research Institute of Electronics, Shizuoka University, Hamamatsu 432, Japan. He is now with the Electrical Communication Laboratories, Nippon Telegraph and Telephone Public Corporation, Tokai-mura, Ibaragi-ken 319-11, Japan.

harmonic components are η_{1n} and ξ_{1n}. Values of k_T, η_{1n}, and ξ_{1n} are determined by the method described in [8].

Results of the derivation give

$$-G_{yy}(R/R') = j \sum_{k_{TH}} \sum_{n=0}^{\infty} \frac{\exp(-j\Gamma_H|z-z'|)}{2\Gamma_H} (\eta_{1n}k_{x1n})^2 \cdot \cos k_{x1n}x \cos k_{x1n}x' \cos \frac{n\pi}{b_3}(y-b_3) \cdot \cos \frac{n\pi}{b_3}(y'-b_3) + j \sum_{k_{TE}} \sum_{n=1}^{\infty} \frac{\Gamma_E \exp(-j\Gamma_E|z-z'|)}{2k^2} \left(\xi_{1n}\frac{n\pi}{b_3}\right)^2 \cdot \cos k_{x1n}x \cos k_{x1n}x' \cos \frac{n\pi}{b_3}(y-b_3) \cdot \cos \frac{n\pi}{b_3}(y'-b_3) \quad (6)$$

for the yy component of the dyadic Green's function which represents the total coupling between the y-pointed current and the ridged waveguide.

Equation (6) suggests that it is appropriate to write the current density in a form

$$\boldsymbol{J}(\boldsymbol{R}) = \begin{cases} \hat{y}J_0 \sum_{n=0}^{\infty} A_n \cos \frac{n\pi}{b_3}(y-b_3)\,\delta(z-0), & -\frac{w}{2} \le x \le \frac{w}{2} \\ 0, & \text{otherwise} \end{cases} \quad (7)$$

where $\hat{y}$ is the y-pointed unit vector and A_n are unknown amplitudes of the spatial harmonic components of the current density in the conductor strip.

Then, we assume a uniform voltage V across the gap since the gap is very small. The gap field, $\boldsymbol{E}_{\text{gap}}(\boldsymbol{R})$, can be written as

$$\boldsymbol{E}_{\text{gap}}(\boldsymbol{R}) = -\hat{y}\frac{V}{g}v(x)v(y)v(z) \quad (8)$$

where

$$v(x) = \begin{cases} 1, & -\frac{w}{2} \le x \le \frac{w}{2} \\ \text{arbitrary}, & \text{otherwise} \end{cases}$$

$$v(y) = \begin{cases} 1, & h-\frac{g}{2} \le y \le h+\frac{g}{2} \\ 0, & \text{along the conductor strip} \end{cases}$$

$$v(z) = \begin{cases} 1, & z = 0 \\ \text{arbitrary}, & z \ne 0. \end{cases}$$

Applying the Lorentz reciprocity theorem to $\boldsymbol{J}(\boldsymbol{R})$, $\boldsymbol{E}(\boldsymbol{R})$, and $\boldsymbol{E}_{\text{gap}}(\boldsymbol{R})$, we have

$$\int_{\text{vol}} \boldsymbol{J}(\boldsymbol{R}) \cdot \boldsymbol{E}_{\text{gap}}(\boldsymbol{R})\,dv = \int_{\text{vol}} \boldsymbol{J}(\boldsymbol{R}) \cdot \boldsymbol{E}(\boldsymbol{R})\,dv. \quad (9)$$

From (9) we can obtain an expression for the driving-point impedance Z_R of the mount defined by $Z_R = V/I$ where I is the total current in the conductor strip using the procedure described in [6]. Results can be written as

$$\frac{1}{Z_R} = \frac{I}{V} = \sum_{n=0}^{\infty} \frac{I_n}{V} = \sum_{n=0}^{\infty} \frac{1}{Z_n} \quad (10)$$

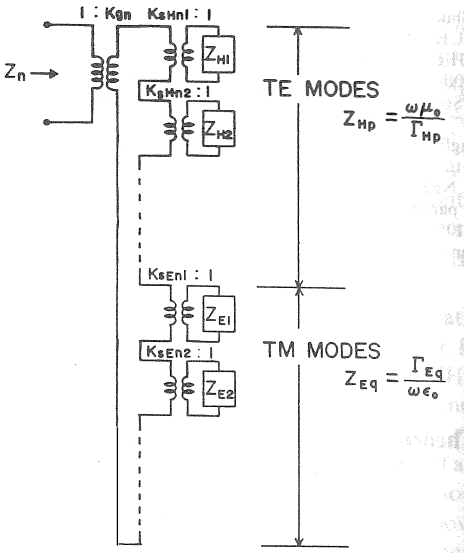

Fig. 2. An equivalent circuit of Z_n.

where

$$Z_n = \frac{V}{I_n} = \frac{1}{K_{gn}^2}\left(\sum_{p=1}^{\infty} K_{sHnp}^2 \frac{\omega\mu_0}{\Gamma_{Hp}} + \sum_{q=1}^{\infty} K_{sEnq}^2 \frac{\Gamma_{Eq}}{\omega\varepsilon_0}\right) \quad (11)$$

with

$$K_{gn} = \sqrt{2}\left\{\frac{2}{b_3(1+\delta_0)}\right\} \cos \frac{n\pi}{b_3}(h-b_3)\left(\frac{\sin\tau_n}{\tau_n}\right) \quad (12)$$

$$K_{sHnp} = (\eta_{1n}k_{x1n})\left(\frac{\sin\theta_n}{\theta_n}\right) \quad (13)$$

$$K_{sEnq} = \left(\xi_{1n}\frac{n\pi}{b_3}\right)\left(\frac{\sin\theta_n}{\theta_n}\right) \quad (14)$$

$$\tau_n = \frac{n\pi}{b_3}\frac{g}{2} \quad (15)$$

$$\theta_n = k_{x1n}\frac{w}{2} \quad (16)$$

and

$$\delta_0 = \begin{cases} 1, & n = 0 \\ 0, & n \ne 0. \end{cases} \quad (17)$$

In (11), Γ_{Hp} and Γ_{Eq} are the propagation constants associated with the pth and the qth lowest order eigenvalues of TE and TM modes, respectively. The factor K_{gn} is the gap coupling factor. Similarly, K_{sHnp} and K_{sEnq} are the conductor-strip coupling factors for the TE and the TM modes, respectively.

Equation (11) can readily be represented by an equivalent circuit as shown in Fig. 2. In view of (10), a parallel connection of Z_n as shown in Fig. 3 gives an equivalent circuit of the driving-point impedance Z_R. Notice that each spatial harmonic component of $\boldsymbol{J}$ couples with all the waveguide modes. This is the consequence of the presence of the ridges in otherwise rectangular waveguide. The equivalent circuit of Fig. 3 reduces, as it should, to the one developed by Eisenhart and Khan in [6] for the rectangular waveguide post-coupling structure when $b_1 \to b_3$ and $b_2 \to 0$, referring to Fig. 1(b).

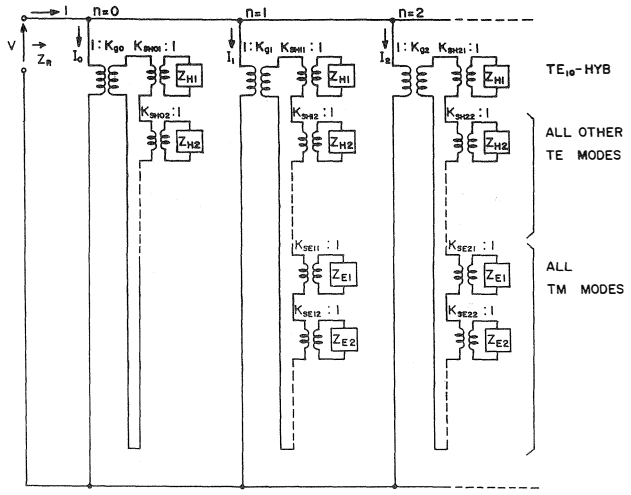

Fig. 3. An equivalent circuit of the driving-point impedance Z_R of the ridged-waveguide mounting structure.

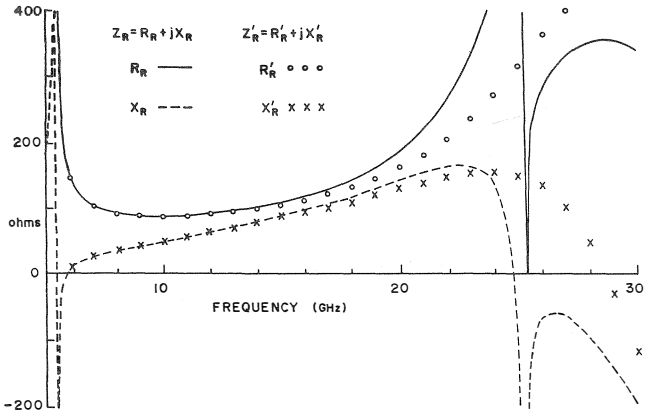

Fig. 4. Frequency characteristics of the real and imaginary parts of $Z_R = R_R + jX_R$ and $Z'_R = R'_R + jX'_R$. Solid curve: R_R; broken curve: X_R; circles: R'_R; crosses: X'_R.

An Example

A typical example is worked out in this section for a conductor strip with $g = 0.5$ mm, $h = b_3/2 = 0.90$ mm, and $w = 1.00$ mm mounted in a ridged waveguide with $a_1 = 1.75$ mm, $a_2 = 7.90$ mm, $b_1 = 4.85$ mm, $b_2 = 3.05$ mm, and $b_3 = 1.80$ mm. The cutoff frequencies of the lowest five modes and the characteristic impedance of the dominant TE_{10}-hybrid mode are listed in Table I.

Numerical evaluation of the driving-point impedance Z_R requires truncation of the summations in (10) and (11) with respect to both n and the number of eigenvalues. In our present example we choose somewhat arbitrarily, but using the discussion given in [6] as a guide, $n \leq 4$ and $f_c \leq 300$ GHz. Results of such calculation are presented in Fig. 4, where the solid and broken curves represent the real and imaginary parts of the driving-point impedance, $Z_R = R_R + jX_R$, respectively. These curves show a remarkably smooth behavior of the driving-point impedance over a range of frequencies from 5.4 to 25.4 GHz, indicating that the ridged-waveguide mounting structure is suitable for wide-band applications.

Of the lowest five modes of the waveguide listed in Table I, only the TE_{10}- and TE_{30}-hybrid modes couple with the current J, because of the waveguide symmetry and our choice of $h = b_3/2$ which makes $Z_n = \infty$ for $n = 1, 3, 5, \cdots$. Thus only the

TABLE I
Rigid Waveguide Characteristics

Mode	Cutoff Freq.	$Z_{0\infty}$
TE_{10}-hybrid	5.4 GHz	120 ohm
TE_{10}-trough	19.2 GHz	—
TE_{20}-hybrid	21.7 GHz	—
TE_{30}-hybrid	25.4 GHz	—
TM_{11}-trough	31.4 GHz	—

(Waveguide dimensions are: $a_1 = 1.75$ mm, $a_2 = 7.90$ mm, $b_1 = 4.85$ mm, $b_2 = 3.05$ mm, and $b_3 = 1.80$ mm)

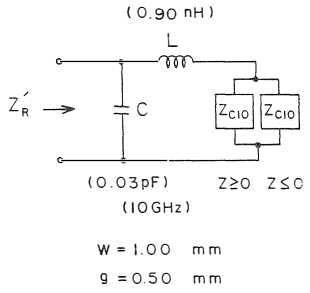

Fig. 5. A simplified equivalent circuit of the driving-point impedance Z'_R. $L = 0.90$ nH and $C = 0.03$ pF evaluated at 10 GHz. $Z_{c10} = Z_{c\infty}(\lambda_g/\lambda) = 120(\lambda_g/\lambda)$.

TE_{10}-hybrid mode propagates while all other modes evanesce, making Z_{H1} resistive, Z_{Hp} $(p \geq 2)$ inductive, and Z_{Eq} $(q \geq 1)$ capacitive at frequencies from 5.4 to 25.4 GHz. The branch impedance for $n = 0$, Z_0, is given by a series connection of a resistance R_R and an inductance L. From (11) through (13), we have

$$R_R = \left(\frac{K_{sH01}}{K_{g0}}\right)^2 \frac{\omega\mu_0}{\Gamma_{H1}} = \frac{1}{2} Z_{c10} \tag{18}$$

where

$$Z_{c10} = (\eta_{1n} k_T b_3)^2 \frac{\omega\mu_0}{\Gamma_{H1}} = Z_{c\infty} \frac{\lambda_g}{\lambda} \tag{19}$$

is the characteristic impedance of the TE_{10}-hybrid mode. For the higher order spatial harmonics, $n \geq 1$, numerical results show that $k_{sHn1} \doteqdot 0$ owing to small values of η_{1n}. In addition, the capacitive reactance dominates over the inductive reactance in each branch impedance Z_n $(n \geq 1)$ over most of the range of frequencies of interest. Exceptions occur when the frequency of operation approaches any of the cutoff frequencies of the higher order modes; Z_n approaches a series resonance. This is reflected in Fig. 4. At frequencies reasonably removed from the cutoff frequencies, the net effect of Z_n $(n \geq 1)$ can be accounted for by a single capacitance shunting across the driving-point terminals. Therefore, the equivalent circuit of Fig. 3 reduces to a simple one given in Fig. 5. Values of L and C evaluated at 10 GHz are 0.90 nH and 0.03 pF, respectively, for our present example.

Using these values and (19), we can calculate the driving-point impedance of the circuit of Fig. 5, $Z'_R = R'_R + jX'_R$, and the results are represented by the circles and the crosses in Fig. 4. Comparison of Z'_R with Z_R justifies the use of the simplified equivalent circuit in practical designs and analyses of the circuits and at the same time points out its limitation.

With regard to the convergence properties of the summations in (10) and (11), we consider that the fundamental aspects of the

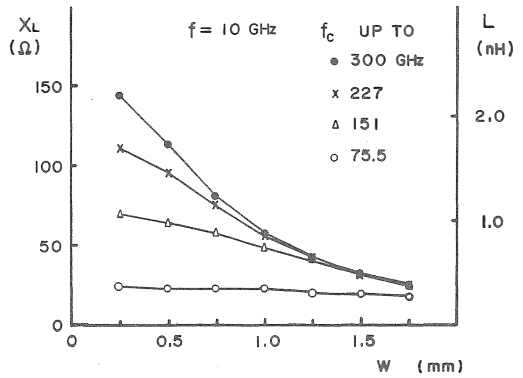

Fig. 6. The conductor strip inductance versus the strip width. The inductance is evaluated by truncating the series at 75.5 GHz through 300 GHz with respect to the eigenvalues and holding $n < 4$ with respect to the spatial harmonics. Ordinate: inductance L, in nanohenries. Abscissa: strip width w, in millimeters.

discussions given in [6] would apply to our problem, and that the series converges for finite w and g. However, our study is incomplete at the time of this writing, and our approach here is to calculate the values of the inductance at various values of the strip width w, using different numbers of the eigenvalues while holding $n \leq 4$ as a test of convergence. A typical set of results are presented in Fig. 6, where all the relevant eigenvalues up to 75.5 GHz through 300 GHz that were detected by a numerical method of scanning on the computer were used. Since the numerical method of scanning has the possibility of leaving out some eigenvalues undetected, precaution is required to include most of the eigenvalues, particularly those of the lower order modes. This is done by checking the number of the eigenvalues detected against that estimated for the through region rectangular waveguide and also by identifying the modes for some twenty lowest order modes.

Fig. 6 shows that truncation at about 300 GHz is acceptable for $w \geq 1.00$ mm. As the width decreases, an increasingly large number of eigenvalues will be required for precision analysis.

Conclusions

A simplified model of the ridged-waveguide mounting structure has been analyzed theoretically. The ribbon-and-pedestal of the microwave diode was represented by an equivalent flat conductor strip having an equivalent width, an infinitesimal thickness, and a gap. The conductor strip was regarded as a small antenna and its driving-point impedance was derived using the induced EMF method. The dyadic Green's function for the ridged waveguide was also derived to facilitate the analysis. The results of the analysis were represented by an equivalent circuit that involved infinite array of transformers representing the couplings between the spatial harmonic components of the current in the conductor strip and the waveguide normal modes. The equivalent circuit was reduced to a simple one convenient for use in practical designs and analyses of microwave circuits involving the mount of this type. Numerical results for a typical example were given to discuss the validity of the theoretical results and also to demonstrate a remarkably smooth behavior of the driving-point impedance of the mount over a frequency range from 5.4 to 25.4 GHz.

The neglect of the package ceramic ring and the lack of theoretical procedure of defining the equivalent width of the flat conductor strip were major shortcomings of the analysis. Experimental measurements were required to supplement these aspects. A through discussion on the convergence properties of the summation was also left for future study. However, the results presented in this short paper will be useful for designs and analyses of various microwave components and circuits involving small devices such as Gunn and IMPATT diodes as well as for characterization of these devices over a wide range of frequencies.

References

[1] D. H. Claxton and P. T. Greiling, "Broad-band varactor-tuned IMPATT-diode oscillator," *IEEE Trans. Microwave Theory Tech.*, vol. MTT-23, pp. 501–504, June 1975.
[2] P. J. Meier, "Integrated fin-line millimeter components," *IEEE Trans. Microwave Theory Tech.*, vol. MTT-22, pp. 1209–1216, Dec. 1974.
[3] S. Mizushina and T. Ohsuka, "The ridged-waveguide-cavity Gunn oscillator for wideband tuning," *IEEE Trans. Microwave Theory Tech.*, vol. MTT-24, pp. 257–259, May 1976.
[4] H. Kondoh, S. Mizushina, and N. Kuwabara, "Broad-band IMPATT and Gunn oscillators with ridged-waveguide cavity," Inst. Elect. Communication Engr. Japan Tech. Rep., MW-76-130, Jan. 1977.
[5] E. Yamashita and J. R. Baird, "Theory of tunnel diode oscillator in a microwave structure," *Proc. IEEE*, vol. 54, pp. 606–611, Apr. 1966.
[6] R. R. Eisenhart and P. J. Khan, "Theoretical and experimental analysis of a waveguide mounting structure," *IEEE Trans. Microwave Theory Tech.*, vol. MTT-19, pp. 706–719, Aug. 1971.
[7] C-T. Tai, *Dyadic Green's Functions in Electromagnetic Theory*. Scranton, PA: Intext Educational Publ., 1971, ch. 5, pp. 69–80.
[8] J. P. Montgomery, "On the complete eigenvalue solution of ridged waveguide," *IEEE Trans. Microwave Theory Tech.*, vol. MTT-19, pp. 547–555, June 1971.

Application of Gratings in a Dielectric Waveguide for Leaky-Wave Antennas and Band-Reject Filters

TATSUO ITOH, SENIOR MEMBER, IEEE

***Abstract*—Grating structures fabricated in inverted-strip dielectric waveguides have been used for the first time as leaky-wave antennas and band-reject filters. They are potentially useful for millimeter-wave integrated circuits. Experimental results agree reasonably well with theoretical predictions.**

I. Introduction

Grating structures are commonly employed in optics as beam couplers [1] and as frequency-sensitive reflectors for distributed-feedback lasers [2]. However, such gratings have not yet been widely used at millimeter wavelengths. Since dielectric waveguides in millimeter-wave integrated circuits (MMIC) are low-frequency replicas of optical waveguide, it is clear that many techniques could be transferred from the optical to the millimeter-wave domain.

This paper reports the first reduction to practice of a frequency-scannable leaky-wave antenna and a band-reject filter made of grating structures implemented in the inverted-strip (IS) dielectric waveguide [3], [4]. The antenna and filter are compatible with, and naturally complement, the directional couplers, oscillators, and phase shifters that have already been developed using dielectric waveguide fabrication techniques [3]–[7]. Grating structures can be easily and economically fabricated in the IS guide. The performance of the antenna and the filter made of gratings can be optimized in a relatively easy and flexible manner. Hence, the development of these devices is likely to contribute to realization

Manuscript received May 19, 1977; revised July 21, 1977.
The author is with the University of Kentucky, Lexington, KY 40506.